Impact of silica nanoparticles on the morphology and mechanical properties of sol-gel derived coatings

Laura VIVAR MORA[1, 4], Alan TAYLOR[2], Shiladitya PAUL[2], Richard DAWSON[3], Chun WANG[4], Wassim TALEB[4], Josh OWEN[4], Anne NEVILLE[4], Richard BARKER[4]

[1]National Structural Integrity Research Centre (NSIRC), United Kingdom mnlvm@leeds.ac.uk
[2]TWI Ltd., United Kingdom
[3] *Lloyd's Register EMEA,* Southampton Technical Support Office, Marine & Offshore, United Kingdom
[4] Institute of Functional Surfaces, School of Mechanical Engineering, University of Leeds, United Kingdom

Abstract:

Although corrosion resistance and mechanical properties of sol-gel coatings have been studied independently, there are limited studies that consider both collectively. However, since any form of mechanical damage could impair the protective function of the coating, it is prudent to consider the mechanical durability of coatings as well as their corrosion resistance. The present work considers the impact of silica nanoparticles on the morphology and mechanical properties of a sol-gel derived coating. The relationships between the results obtained from tests such as atomic force microscopy (AFM), nanoindentation or erosion test with previously reported corrosion results obtained via salt spray or electrochemical impedance spectroscopy (EIS) are discussed. Results show that reinforcing a sol-gel coating with silica nanoparticles and, particularly, functionalised silica nanoparticles led to coatings with improved mechanical properties and enhanced erosion impact resistance. The role of nanoparticles on improving mechanical properties and corrosion resistance, which is of importance within the coating industry, is discussed.

Highlights:

- Effect of SiO_2 on morphology and mechanical properties in a sol-gel coating was studied
- SiO_2 surface treatment improved mechanical durability and corrosion resistance
- Importance of studying mechanical and corrosion resistance properties of coatings has been proved

Keywords:

sol-gel coatings, silica nanoparticles, nanoparticle surface treatment, corrosion protection, mechanical durability

1. Introduction

The use of nanomaterials in the formulation of coatings is very promising [1]. Nanoparticles can be added to coatings to provide various new functionalities and advantages. The choice of which nanoparticle is used depends on the desired property. Nano-sized pigments and fillers, nanopolymer dispersions, and nano-additives are now commercially available and many more are in the development stage, designed as a consequence of the current advances in nanotechnology. Nanotechnology is used in many different industries and for many different applications. It can be used to develop nanoparticles which can deliver drugs to diseased cells [2, 3] enhance the efficiency of solar cells [4], produce coatings with superior mechanical properties [5-12], or enable nano-additives for use in anti-corrosion coatings [13-19].

Many studies have been carried out to demonstrate the influence of nanoparticles on corrosion resistance of coatings on steel [13-19] or light metals [20-22]. There are many examples in the literature of the use of a range of the incorporation of fillers to improve coating properties. These can be categorised as additives with layer structures [23-29] or by functional attribute such as barrier properties [30-32], corrosion inhibition [14, 15, 33, 34] or mechanical performance [32, 35, 36]. Similarly, the number of publications on the influence of mechanical properties of coatings has been growing [37]. However, whilst few researchers have developed an understanding of the correlation between durability, morphology and functional performance [38] it is an area of active interest. The approaches reported to date essentially describe a combinatorial approach were available materials are combined in various ways and the properties of the resultant material evaluated. The complexity of matrix-filler-processing options make an holistic approach to the identification of the most effective combination extraordinary difficult. The fact that there is no meaningful definition on how to describe organic-inorganic hybrids illustrates the challenge, although both Novak [39] and Sanchez [40] have suggested categorisation definitions.

Incorporation of nanoparticles in a polymer matrix modifies the physical and mechanical properties of the matrix leading to some new characteristics which may improve the performance of the coating if added in the correct manner with an appropriate quantity. The final properties are affected by many factors and the interaction between the nanoparticles and the matrix as well as the degree of dispersion play a critical role [41-44]. Understanding the consequences of nanoparticles on durability and mechanical properties is important to ensure adequate and reliable corrosion protection. There are many factors affecting degradation of coatings and corrosion, some of them are summarised in Figure 1.

For many applications, such as offshore, coatings need to provide not only effective corrosion protection but be robustly resilient. Mechanical damage can impair the protection characteristics of barrier coatings and compromise materials' integrity affecting assets, environment and people. Thus, it is important to evaluate both the mechanical durability and corrosion resistance of coatings.

Sol-gel based coatings, despite decades of research and many potential advantages, have not been as widely adopted as they could [45]. Several groups have studied the mechanical properties of these types of coatings on different substrates such as plastics, glass, aluminium or metals [5, 11, 46-52]. Even though mechanical properties are dependent on many factors, such as the nature of the precursors, the reaction parameters or the coating deposition and curing, an improvement has been observed when nano-additives are incorporated into sol-gel matrices [6, 41].

One of the challenges with the addition of nanoparticles is the dispersion into the hybrid matrix. If the nanoparticles agglomerate the result is coatings with poor mechanical properties [37]. In order to overcome this, the surface of nanoparticles can be modified to improve their interaction with the matrix [43, 44, 52, 53]. Our previous work [54] showed that the surface treatment of silica nanoparticles provides greater compatibility with the sol-gel derived matrix, compared with unfunctionalised silica added to the same matrix, leading

to a more homogeneous and flexible coating, which is in line with other work [43, 44, 52, 53].

Some important parameters to evaluate mechanical properties of coatings are hardness, elastic modulus and fracture toughness. Nanoindentation and scratch testing are the most widely used techniques to measure mechanical properties of thin coatings. Their applicability and practical use to evaluate sol-gel coatings and nanoparticle-loaded sol-gel coatings has been demonstrated [55].

This work reported herein in part of a later programme attempting to establish some preliminary design rules of the fabrication of silica nanoparticles, their incorporation into coatings and resin systems and their subsequent impact on final material properties. The specific focus of this work is to develop an understanding the impact of unfunctionalised and functionalised silica nanoparticles on the mechanical properties and durability of a sol-gel derived coating. We relate this to our previous work [54] which showed that the addition of silica nanoparticles helped increase the coating homogeneity, which led to an improvement in coating performance. However when these nanoparticles were surface treated, an enhancement in nanoparticle distribution and coating homogeneity was observed possibly due to a stronger nanoparticle-matrix interface, which led to an increase in corrosion resistance. The aim of this work is to understand the impact of these silica nanoparticles on the mechanical properties of the loaded polysiloxane coating, and determine whether these characteristics are improved in conjunction with the corrosion resistance observed and reported previously. We will report on the particle distribution and morphological aspects in a later publication.

2. Experimental

2.1 Materials synthesis

Q-panels (Q-Lab Company, UK), grade S-46 (SAE 1008/1010, mild steel, with a chemical composition of 0.60% max manganese, 0.15% max carbon, 0.030% max phosphorus, 0.035

% max sulfur), ground on one side with dimensions of 0.8 x 102 x 152 mm were used as the substrate. TES40, an oligomeric form of TEOS (tetraethylorthosilicate), and 3-glycidoxypropyltrimethoxysilane (GPTMS) precursors were supplied by Silanes and Silicones Manufacturing, UK. The synthesis of 25 nm diameter spherical silica nanoparticles was carried out at TWI Ltd., Cambridge, using a standard Stöber method [56]. As this Stöber silica is dispersed in a liquid phase, this makes these nanoparticles easily manageable for any additional treatment. In this work, as-synthesised silica was functionalised with GPTMS and had a nanoparticle size of ~ 30 nm.

The coating matrix was created using sol-gel chemistry with TES40 and GPTMS used as precursors (in a TES40/GPTMS molar ratio of 1:1.8), in the presence of acidic catalyst of HCl with water and Industrial Methyl Spirit (IMS) as solvents, where then silica nanoparticles were incorporated. The synthesis and coating preparation of the sol-gel based matrix and the silica nanoparticles, both unfunctionalised and functionalised with GPTMS, has been reported previously [54]. Prior to coating deposition, steel panels were cleaned with IMS to remove grease and/or contaminants and then the coatings were applied manually using 50 μm wire wound bars on to the steel panels (Elcometer, Manchester, UK). The coated samples were then dried and cured at 90 °C for 2 h in an oven, afterwards the coating thickness was measured to be 20–40 μm [54].

Both types of silica nanoparticles, unfunctionalised and functionalised, were incorporated into the coating matrix to a 10 wt. % loading level.

2.2 Coating characterisation

Adhesion of the coating to the substrate was measured by the cross-cut tape test method following ASTM D3359 - 09e2, which specifies a procedure for assessing the adhesion resistance between coatings and substrates when a lattice pattern is cut into the coating. Adhesion is rated from 5B to 0B depending on the extent of loss of the coating with 5B indicating no loss and so excellent adhesion.

Roughness measurements were obtained using an Atomic Force Microscope (AFM - Dimension Icon from Bruker, Germany) operating in Peakforce Quantitative Nano-mechanical mapping mode using a silicon tip on nitride cantilever probeq (nominal spring constant 0.4974 N/m, nominal resonance frequency of 70 kHz).

The mechanical properties of the coatings were analysed by means of nanoindentation on 1 cm x 1 cm sectioned flat samples, using a Berkovich diamond indenter tip. The indenter has an angle of 65.3° between the tip axis and the faces of a triangular pyramid. Before testing, the machine was calibrated according to ISO-14577. Indentation was load controlled to a maximum load of 1 mN. The loading rate was 0.01 mN/s and the unloading rate 0.1 mN/s. The indentation depth was less than one tenth of the coating thickness, 20-40µm as reported in [54], in order to measure the properties of the coating without significant interference of the substrate [55].The data was analysed using a power law fitting procedure by Oliver and Pharr [57], to derive the hardness and modulus values. Since this analytical technique just provides the reduced modulus, E_r, the following equation (1) was used to obtain the Young's modulus, E:

$$\frac{1}{E_r} = \frac{(1-\nu_i^2)}{E_i} + \frac{(1-\nu^2)}{E} \qquad (1)$$

where ν_i is the indenter Poisson's ratio and has a value of 0.07, E_i is the indenter modulus and is equal to 1140 for diamond and ν is the Poisson's ratio associated with the sol-gel coating and it is estimated to be 0.225 [55].

The coatings were also evaluated by electrochemical measurements, which were performed using a conventional three-electrode cell with 3.5 wt.% NaCl electrolyte at ambient conditions. The working electrode was the coated sample (exposed area 15.2 cm^2), the reference electrode was Ag/AgCl (4M KCl) type and the counter electrode was a Pt/Ti wire. The polarisation was carried out in sets of 3 samples for each coating system. Experiments were performed in 3.5 % NaCl solution using an Ivium pocketSTAT (Ivium,

Netherlands). Initial open circuit potential, E_{oc}, was taken and then the polarisation was acquired with a scan rate of 0.167 mV/s in the region from – 20 mV vs E_{oc}.

2.3 Erosion resistance

Measurement of the resistance of the candidate coatings to sand erosion was undertaken using a submerged impingement jet [58]. The submerged impingement jet reservoir was filled with 50 L of water and 1000 mg/L of sand that was recirculated through a dual nozzle arrangement onto the flat specimens at an angle of 90°, positioned 5 mm from the exit of the nozzle. Spherical sand particles were used with an average particle diameter of 250 μm. The solution was sparged with nitrogen (N_2) during the test and for a minimum of 12 hours prior to starting the test, to reduce the dissolved oxygen concentration in the solution to below 50 ppb. Tests were conducted in 3 different specimens for each formulation at a flow velocity of 15 m/s and a temperature of 25 °C. The mass of the samples was measured before and after the test using a mass balance accurate to 1 μg. After the erosion tests, samples were profiled using a Bruker NPFLEX 3D optical profiler.

3. Results and discussion

3.1 Coating morphology

An important parameter influencing mechanical properties of any coating is the interface between the substrate and the coating and particularly the adhesion of the coating to the substrate. It was observed that the cross hatch squares on the coating matrix showed no cracking or chipping and the coating was rated as 5B. Introduction of nanoparticles can lead to an increase in hardness and rigidity of the coating, however coatings with unfunctionalised as well as functionalised nanoparticles didn’t show any cracking or chipping, the edges of the cuts are completely smooth without any lattice detached so they were also rated as 5B.

An increase in coating homogeneity can be seen in the AFM topography images in Figure 2, where a smoother surface structure is observed for the coating with functionalised nanoparticles. This is also reflected on the roughness values gathered after AFM analysis,

which was performed on an area of 10 µm x 10 µm for all formulations. The average roughness, R_a, and the root mean square roughness, R_q, represented in Figure 3 were used to characterise surface topography.

It can be observed from Figure 3 that the roughness values for the coating matrix and the matrix with unfunctionalised silica show similar values. A notable decrease in both R_a and R_q is recorded when functionalised silica nanoparticles are incorporated into the coating matrix. This is an indication that roughness is related with nanoparticle distribution: the coating with non-functionalised silica nanoparticles presented some degree of agglomeration and nanoparticles concentrated at particular regions which made this coating rougher. Conversely, the introduction of functionalised silica to the sol-gel based matrix showed no agglomeration of nanoparticles leading to smallest surface roughness. This decrease in roughness could be explained by the surface functionalisation of the silica surface which made the nanoparticles more compatible with the matrix improving the dispersion and homogeneity of the formulation.

3.2 Mechanical performance

Important parameters describing the mechanical properties of coatings are the hardness, H, and Young's modulus, E, which were obtained with nanoindentation. Hardness is a measure of material resistance to plastic deformation and depends on the rigidity of its bonding network while the Young's modulus is a measure of the material resistance to elastic deformation and thus, related to the bond strength between atoms.

Figure 4 shows the hardness and Young's modulus values for all formulations. A potential increase of hardness with the addition of non-functionalised silica nanoparticles can be noticed, hardness value that is even higher when the functionalised silica is incorporated to the matrix.

A similar trend is observed in Figure 4 for the Young's modulus, where again the addition of silica led to an increase in modulus. This was expected since the modulus of silica, E = 70

GPa [59], is much greater than the base matrix. The increase in modulus was even more noticeable when the nanoparticles were surface treated. This could be explained by the better compatibility between the matrix and the functionalised nanoparticles leading to a more uniform distribution giving a more resistant material to elastic deformation. This enhanced compatibility is due to the silylation used for the surface modification, where the glycidoxypropyl groups from the GPTMS may be grafted onto the silica nanoparticles which then are incorporated into the polymer network through covalent bonds. The formation of covalent bonds between the nanoparticles and the polymer matrix can favour crosslinks enhancing the network density of the final material [43].

The ratio of hardness to Young's modulus, H/E, also termed brittleness index has been shown to be proportional to the resistance of wear [52, 60, 61]. It can be observed from Figure 5 how the addition of silica produced a decrease in the brittleness index, with the coating containing functionalised silica nanoparticles presenting the lower value. This is in line with the previous results showing that surface treatment increased crosslinking and compatibility matrix-nanoparticles creating a less brittle and more durable coating.

A comparison of the effect of the incorporation of both non-functionalised as well as epoxy-functionalised silica nanoparticles into the based matrix on hardness, elastic modulus and brittleness index is shown in Table 2. The incorporation of functionalised silica led to increased hardness and elasticity by a factor of 1.5 and 1.8 relatively compared with the non-functionalised, while the brittleness decreased by a factor of 1.2. Thus, the incorporation of functionalised silica nanoparticles led to harder, more elastic coatings whilst also decreasing brittleness.

As mentioned earlier, fracture toughness is also an important parameter to characterise mechanical properties of coatings. Fracture toughness, K_c, measures the ability of a material to resist crack propagation and can be estimated by using the following relation [62]:

$$K_c = \alpha\,(P/c^{3/2})(E/H)^{(1/2)} \qquad (2)$$

where α is a constant which depends on the geometry of the indenter (0.016 for a Berkovich type indenter), P is the peak indentation load and c is crack length. In this equation (2), $P/c^{3/2}$ refers to the ability of the materials to resist crack propagation and $E/H^{1/2}$ refers to the potential to resist a possible fracture [63]. Thus, the ratio $(E/H)^{1/2}$ will be used to indicate the comparative toughness of these materials in this work. Figure 6 shows an increase in toughness from the matrix to the coatings with silica nanoparticles, presenting higher toughness the coating with functionalised silica. This increased toughness could be a result of the decreased defect density and increased chemical bonding.

As mentioned earlier, it is important to evaluate and correlate mechanical durability with corrosion resistance to assess the reliability of coatings used in industrial applications. Results indicate that the corrosion behaviour is not only dependent on coating quality but also on roughness. An increase in surface roughness has been related to increased corrosion rate and this behaviour has been reported by other authors [64, 65]. Roughness also results in the reduction of effective thickness and this may well result in the reduction of water uptake time.

3.3 Electrochemical behaviour

To determine the defect density of the coatings, potentiodynamic polarisation was carried out once the 48 h EIS test was completed. Figure 7 shows the potentiodynamic polarisation diagram for all coatings in 3.5 wt.% NaCl solution at ambient temperature. A change of potential to more positive values can be observed from the matrix to the coatings with silica nanoparticles. This change is more noticeable for the coating containing functionalised silica nanoparticles. An increase in anodic current of one order of magnitude can be also observed from the matrix to the coating containing non-functionalised silica, and similarly, the coating with functionalised silica presented an anodic current one order of magnitude higher than the coating with non-functionalised silica.

Corrosion current density is usually associated with defect density, which is related to the pinholes or imperfections which can be form during coating deposition and curing. Figure 8 shows the defect density values, which were calculated using the following relation [66]:

$$P = \frac{R_{ps}}{R_p} \times 10^{-\frac{|\Delta E_{corr}|}{\beta_a}} \qquad (3)$$

where P is the defect density, R_{ps} is the polarisation resistance of the substrate without any coating, R_p is the polarisation resistance for each coating, ΔE_{corr} is the corrosion potential difference between the substrate and the coating layer, and β_a is the anodic Tafel slope. Figure 8 indicates how the nanoparticles reduce the coating defect density which in turn influences the corrosion protection offered by the coating.

Figure 9 is a representation of the influence of roughness (R_a) on defect density, water uptake and corrosion resistance. Previous work [54] showed the evolution of the water uptake and the corrosion resistance over time. R_{corr} is the corrosion resistance of the coatings (in Ω.cm) and Q_{coat} is the coating capacitance (in F/cm), which can be associated with water uptake or entry of the electrolyte into the coating [67, 68]. Our previous work [54] showed that the addition of silica nanoparticles led to lower values of coating capacitance compared with the matrix alone, but with the incorporation of functionalised silica Q_{coat} values were even lower. Regarding the corrosion resistance, it was observed that the coating with functionalised silica nanoparticles presented the highest values of R_{corr}.

Figure 9 shows that the coating matrix presents higher roughness and higher defect density than the coatings with nanoparticles, these defects could act as gateways to the entry of the electrolyte in the network structure leading to increased water uptake and less protective properties. The introduction of unfunctionalised silica nanoparticles lead to a decrease in roughness, defect density and water uptake (Q_{coat}) which increases the resistance of the coating to corrosion (R_{corr}). However, when functionalised silica is incorporated to the sol-gel derived matrix, a further enhancement is observed, presenting this coating with the highest

corrosion resistance values, as reported previously [54]. These results are in agreement with data found in the literature where samples with higher roughness led to less protective coatings [64, 69].

Sol-gel coatings usually possess pores or defects after curing and the addition of silica nanoparticles can assist in filling or reducing the potential for stress related cracking, but also can enhance the network density and the compatibility between the nanoparticles and the hybrid matrix which could be a possible mechanism for the improvement of the corrosion resistance. While lowering the defect density, the water uptake will decrease due to the reduction in the ion-conducting paths in the coating which will help to improve coating microstructure and have a positive effect on corrosion protection.

However, this reduction in stress related cracking and defect density is not just influencing corrosion features but also this improved coating microstructure is having an effect on the fracture resistance and mechanical properties of the resulting coatings, as can be observed from Figure 10. Figure 10 shows a diagram used to evaluate both mechanical and corrosion protection characteristics. It can be noticed that the improvement in mechanical properties with the addition of functionalised silica: decreased roughness, increased hardness, increased Young's modulus, decreased brittleness and increased toughness, have a positive impact on the corrosion protection of these coatings. The sol-gel based matrix presented higher degree of roughness and also higher defect density which can affect negatively fracture resistance since defects can act as flaws causing stress and lowering fracture resistance. The incorporation of silica nanoparticles, particularly the functionalised silica, showed lower values of both roughness and defect density and improved mechanical properties. Both the hardness and elasticity of the coatings with functionalised silica nanoparticles were increased possibly due to the enhanced nanoparticle distribution and network density which led to a more resistant material. Furthermore, the incorporation of functionalised silica showed to decrease the defect density and increase the toughness. This increase in toughness is also

reflected in the decrease in coating brittleness. The decreased stress in the coating and the enhanced chemical bonding between the nanoparticles and the matrix would have contributed to this, which would have led also to both lower water uptake and higher corrosion resistance properties.

3.4 Erosion

However, other aspects can affect coating durability. Sand and rain can cause erosion of coatings reducing its durability and applicability. Thus, wear resistance of the coatings has been studied by erosion tests. Assessment of the resistance of all coatings to sand erosion by measuring mass loss after testing is shown in Figure 11. The addition non-functionalised and functionalised silica nanoparticles improved impact resistance showing these coatings superior erosion resistance compared to the coating matrix. The mass loss was reduced by approximately 80% with the addition of silica nanoparticles, with the functionalised silica showing slightly enhanced erosion resistance than the non-functionalised sample.

Surface morphology images of the coatings after erosion tests are shown in Figure 12. It can be observed that the coating matrix had multiple areas of the coating removed, with some of the removal in regions where there were very few impacts from sand particles. This could be explained due to the higher brittleness of the coating matrix which could have facilitated the removal of the coating. However the addition of non-functionalised and functionalised silica nanoparticles showed similar removal which was just concentrated at the impinging area.

Profilometry images were taken in order to have a better idea of the surface morphology and coating removal from erosion tests. Figure 13 showed the surface profiles of all coating samples. It can be seen that the coating matrix loses significantly more material than those coatings with silica nanoparticles. This could be explained due to the improved mechanical properties with the addition of silica. The wear resistance of coatings can be related to the hardness and brittleness index of the materials. The incorporation of silica to the sol-gel

matrix led to increased hardness and elasticity and decreased brittleness index, which was even more noticeable with the incorporation of functionalised silica. This would mean that this coating is more resistance to deformation and more durable which is in line with the erosion tests results and would explain the decrease on impact damage for the coating with functionalised silica nanoparticles.

The coating with functionalised silica also produced the lowest mass loss after these tests and it can be seen that this coating did not show any noticeable change in appearance, the characteristic transparency remained after the end of the test.

4. Conclusions

In this paper we have studied both the mechanical properties and corrosion resistance characteristics of a sol-gel based coating with both unfunctionalised as well as functionalised silica nanoparticles.

This study has shown that the introduction of silica nanoparticles to a sol-gel based coating have improved the mechanical properties and also the corrosion resistance. However when these silica nanoparticles were surface treated, the defect density of the coating further decreased and the mechanical properties (hardness, elastic modulus, brittleness and fracture toughness) improved and led to more durable and corrosion resistant coating.

Furthermore, reinforcing the sol-gel matrix with silica nanoparticles increases the erosion resistance of the coatings and led to a mass loss reduction of around 80 %.

It has been demonstrated that mechanical properties and corrosion resistance parameters can be correlated, which is of high importance when looking for industrial application of coatings.

Acknowledgements

The author would like to thank the Lloyd's Register Foundation for sponsoring this PhD research and the FCR Team at TWI for their support.
[Lloyd's Register Foundation] is a charitable foundation, helping to protect life and property by supporting engineering-related education, public engagement and the application of research.

References

[1] M. Balasubramanian, Nanocomposites, in: Composite materials and processing, Taylor & Francis Group, Boca Raton, 2014

[2] R. Xu, G. Zhang, J. Mai, X. Deng, V. Segura-Ibarra, S. Wu, J. Shen, H. Liu, Z. Hu, L. Chen, Y. Huang, E. Koay, Y. Huang, J. Liu, J. E. Ensor, E. Blanco, X. Liu, M. Ferrari, H. Shen, An injectable nanoparticle generator enhances delivery of cancer therapeutics, Nat. Biotechnol. 34 (2016) 414–418.

[3] Z. Gu, T. T. Dan, M. Ma., B. C. Tang, H. Cheng, S. Jiang, Y. Dong, Y. Zhang, D. G. Anderson, Glucose-Responsive Microgels Integrated with Enzyme Nanocapsules for Closed-Loop Insulin Delivery, ACS Nano, 7 (8) (2013) 6758-6766.

[4] S. Sagadevan, Recent trends on nanostructures based solar energy applications: A review, Rev. Adv. Mater. Sci. 34 (2013) 44-61.

[5] D. Kumar, X. Wu, Q. Fu, J.W.C. Ho, P.D. Kanhere, L. Li, Z. Chen, Development of durable self-cleaning coatings using organic-inorganic hybrid sol-gel method, Appl. Surf. Sci. 344 (2015) 205–212.

[6] J. Wang, G. Wu, J. Shen, T. Yang, Q. Zhang, B. Zhou, Z. Deng, B. Fan, D. Zhou, F. Zhang, Scratch-Resistant Improvement of Sol-Gel Derived Nano-Porous Silica Films, J. Sol-Gel Sci. Technol. 18 (2000) 219–224.

[7] Y. Bautista, J. Gonzalez, J. Gilabert, M.J. Ibañez, V. Sanz, Correlation between the wear resistance, and the scratch resistance, for nanocomposite coatings, Prog. Org. Coatings. 70 (2011) 178–185.

[8] R. Eslami-Farsani, H. Khosravi, S. Fayazzadeh, Using-3-glycidoxypropyltrimethoxysilane functionalized SiO_2 nanoparticles to improve flexural properties of glass fibers/epoxy grid-stiffened composite panels, Int. J. Chem. Mol. Nucl. Mater. Metall. Eng. 9 (2015) 1377–1380.

[9] S. Kang, S. Hong, C.R. Choe, M. Park, S. Rim, J. Kim, Preparation and characterization of epoxy composites filled with functionalized nanosilica particles obtained via sol-gel process, Polymer, 42 (2001) 879–887.

[10] Y. Han, A. Taylor, and K. M. Knowles, Characterisation of organic-inorganic hybrid coatings deposited on aluminium substrates, Surf. Coatings Technol. 202 (9) (2008) 1859–1868.

[11] Y. Han, A. Taylor, and K. M. Knowles, Scratch resistance and adherence of novel organic-inorganic hybrid coatings on metallic and non-metallic substrates, Surf. Coatings Technol. 203 (19) (2009) 2871–2877.

[12] N. G. Salleh, H. J. Glasel, R. Mehnert, Development of hard materials by radiation curing technology, Radiat. Phys. Chem. 63 (2002) 475-479.

[13] M.L. Zheludkevich, R. Serra, M.F. Montemor, I.M. Miranda Salvado, M.G.S. Ferreira, Corrosion protective properties of nanostructured sol-gel hybrid coatings to AA2024-T3, Surf. Coatings Technol. 200 (2006) 3084–3094.

[14] M.F. Montemor, M.G.S. Ferreira, Cerium salt activated nanoparticles as fillers for silane films: Evaluation of the corrosion inhibition performance on galvanised steel substrates, Electrochim. Acta. 52 (2007) 6976–6987.

[15] M.F. Montemor, R. Pinto, M.G.S. Ferreira, Chemical composition and corrosion protection of silane films modified with CeO_2 nanoparticles, Electrochim. Acta. 54 (2009) 5179–5189.

[16] M. Zaharescu, L. Predoana, A. Barau, D. Raps, F. Gammel, N.C. Rosero-Navarro, Y. Castro, A. Durán, M. Aparicio, SiO_2 based hybrid inorganic–organic films doped with TiO2–CeO2 nanoparticles for corrosion protection of AA2024 and Mg-AZ31B alloys, Corros Sci. 51 (2009) 1998-2005.

[17] M.L. Zheludkevich, R. Serra, M.F. Montemor, K.A. Yasakau, I.M.M. Salvado, M.G.S. Ferreira, Nanostructured sol-gel coatings doped with cerium nitrate as pre-treatments for AA2024-T3 Corrosion protection performance, Electrochim. Acta. 51 (2005) 208–217.

[18] R.N. Peres, E.S.F. Cardoso, M.F. Montemor, H.G. de Melo, A. V. Benedetti, P.H. Suegama, Influence of the addition of SiO_2 nanoparticles to a hybrid coating applied on an AZ31 alloy for early corrosion protection, Surf. Coatings Technol. 303 (2016) 372–384.

[19] I. Santana, A. Pepe, E. Jimenez-Pique, S. Pellice, I. Milosev, S. Ceré, Corrosion protection of carbon steel by silica-based hybrid coatings containing cerium salts: Effect of silica nanoparticle content, Surf. Coatings Technol. 265 (2015) 106–116.

[20] S. Kozhukharova, V. Kozhukharova, M. Schemb, M. Aslanb, M. Wittmarb, A. Wittmarb, M. Veithb, Protective ability of hybrid nano-composite coatings with cerium sulphate as inhibitor against corrosion of AA2024 aluminium alloy, Prog. Org. Coat., 73 (2012) 95– 103.

[21] A. A. Salve1, S. Kozhukharov, J. E. Pernas, E. Matter, M. Machkova, A comparative research on hybrid and hybrid nano-composite protective primary coatings for AA2024 aircraft alloy, J. Univ. Chem. Tech. Metal., 47 (3) (2012) 319-326.

[22] N. N. Voevodin, J. W. Kurdziel, R. Mantz. Corrosion protection for aerospace aluminum alloys by Modified Self-assembled NAnophase Particle (MSNAP) sol–gel, Surf. Coatings Technol., 201 (2006) 1080–1084.

[23] J. Yang, L. Bai, G. Feng, X. Yang, M. Lv, C. Zhang, H. Hu, X. Wang. Thermal reduced graphene based polyethylene vinyl alcohol nanocomposites: enhanced mechanical properties, gas barrier, water resistance, and thermal stability, Ind. Eng. Chem. Res., 52 (2013) 16745-16754.

[24] C. K. Lam, H. Cheung, K. Lau, L. Zhou, M. Ho, D. Hui, Cluster size effect in hardness of nanoclay/epoxy composites, Composites Part B: Engineering., 36 (3) (2005) 263-269.

[25] D. Burgentzle, J. Duchet, J. F. Gerard, A. Jupin, B. Fillon. Solvent-based nanocomposite coatings: I. Dispersion of organophilic montmorillonite in organic solvents, J. Colloid Interface Sci., 278 (1) (2004) 26-39.

[26] C. Deshmane, Q. Yuan, R. S. Perkins, R. D. K. Misra. On striking variation in impact toughness of polyethylene-clay and polypropylene-clay nanocomposite systems: the effect of clay-polymer interaction, Mater. Sci. Eng. A., 458 (2007) 150-157.

[27] L. Moyo, W. W. Focke, D. Hedenreich, F. J. W. J. Labuschagne, H. J. Radusch. Properties of layered double hydroxide micro- and nanocomposites, Mater Res Bull., 48 (2013) 1218-1227.

[28] S. Pradhan, F. R. Costa, U. Wagenknecht, D. Jehnichen, A. K. Bhowmick, G. Heinrich. Elastomer/LDH nanocomposites: Synthesis and studies on nanoparticle dispersion, mechanical properties and interfacial adhesion, Eur. Polym. J., 44 (10) (2008) 3122-3132.

[29] H. B. Hsueh, C. Y. Chen. Preparation and properties of LDHs/epoxy nanocomposites, Polymer, 44 (2003) 5275-5283.

[30] G. X. Shen, Y. C. Chen, L. Lin, C. J. Lin, D. Scantlebury. Study on a hydrophobic nano-TiO2 coating and its properties for corrosion protection of metals, Electrochim. Acta., 50 (2205) 5083-5089

[31] L. Bamoulid, M. T. Maurette, D. De Caro, A. Guenbour, A., Ben Bachir, L. Aries, S. El Hajjaji, F. Benoit-Marquie, F., Ansart. An efficient protection of stainless steel against corrosion: combination of a conversion layer and titanium dioxide deposit, Surf. Coatings Technol., 202 (20) (2008) 5020-5026.

[32] S.A. Khorramie, M. A. Baghchesara, R. Lotfi, S. M. Dehagi. Synthesis of ZrO2 nanoparticle by combination of sol-gel auto-combustion method-irradiation technique, and preparation of Al-ZrO2 metal matrix composites, Int. J. Nano Dimens., 2 (4) (2012) 261-267.

[33] R. Z. Zand, V. Flexer, M. De Keersmaecker, K. Verbeken, A. Adriaens, Effects of activated ceria and zirconia nanoparticles on the protective behaviour of silane coatings in chloride solutions, Int. J. Electrochem. Sci., 10 (2015) 997-1014.

[34] B. Echalier, 2005. Nanoparticles of Cerium Oxide – Application to coatings technologies. In: Nano and Hybrid Coatings conference, January 2005, Manchester. [Online] Available from: http://www.pcimag.com/articles/83469-nanoparticles-of-cerium-oxide-application-to-coatings-technologies

[35] S. Logothetidis, A. Laskarakis, S. Kassavetis, S. Lousinian, C. Gravalidis, G. Kiriakidis, Optical and structural properties of ZnO for transparent electronics, Thin Solid Films., 516 (7) (2008) 1345-1349.

[36] M. D. Clark, M. R. Maschmann, R. J. Patel, B. J. Leever, Scratch resistance and durability enhancement of bulk heterojunction organic photovoltaics using ultra-thin alumina layers. Sol. Energy Mater Sol. Cells., 128 (2014) 178-183.

[37] D. Guo, G. Xie, J. Luo, Mechanical properties of nanoparticles: basics and applications, J. Phys. D: Appl. Phys., 47 (1) (2014).

[38] A.M. Wojdyla, A.Taylor, G.G. Durand, I. W. Boyd, New assessment criteria for durability evaluation of highly repellent coatings, Wear 390-391 (2017) 49-60.

[39] B. M. Novac, Hybrid nanocomposite materials – between inorganic glasses and organic polymers, Adv. Mater., 5 (6) (1993) 422-433.

[40] C. Sanchez, L. Rozes, F. Ribot, C. Laberty-Rober, D. Grosso, C. Sassoye, C., Boissiere, L. Nicole, "Chimie douce": A land of oportunities for the designed construction of functional inorganic and hybrid organic-inorganic nanomaterials, C. R. Chim.,13 (2010) 3-39.

[41] I.A. Rahman, V. Padavettan, Synthesis of silica nanoparticles by sol-gel: size-dependent properties, surface modification, and applications in silica-polymer nanocomposites. A review, J. Nanomaterials 2012, Article ID 132424, (2012).

[42] S. Kang, S. Hong, C.R. Choe, M. Park, S. Rim, J. Kim, Preparation and characterization of epoxy composites filled with functionalized nanosilica particles obtained via sol-gel process, Polymer, 42 (2001) 879–887.

[43] F. Bauer, V. Sauerland, H. Glasel, H. Ernst, M. Findeisen, E. Hartmann, H. Langguth, B. Marquardt, R. Mehnert, Preparation of scratch and abrasion resistant polymeric nanocomposites by monomer grafting onto nanoparticles, 3[a] Effect of filler particles and grafting agents, Macromol. Mater. Eng. 287 (2002) 546-552.

[44] F. Bauer, H. Ernst, D. Hirsch, S. Naumov, M. Pelzing, V. Sauerland, R. Mehnert, Preparation of scratch and abrasion resistant polymeric nanocomposites by monomer grafting onto nanoparticles, 5[a] Application of mass spectroscopy and atomic force microscopy to the characterisation of silane-modified silica surface, Macromol. Chem. Phys. 205 (2004) 1587-1593.

[45] M. Rostami, Z. Ranjbar, M. Mohseni,, Investigating the interfacial interaction of different aminosilane treated nano silicas with a polyurethane coating, Appl. Surf. Sci. 257 (2010) 899-904.

[46] R. B. Figueira, I. R. Fontinha, C. J. R. Silva, E. V. Pereira, Hybrid sol-gel coatings: Smart and Green materials for corrosion mitigation, Coatings, 6 (2016) 12.

[47] J. Ballarre, E. Jimenez-Pique, M. Anglada. S. A. Pellice, A. L. Cavalieri, Mechanical characterization of nano-reinforced silica based sol–gel hybrid coatings on AISI 316L stainless steel using nanoindentation techniques, Surf. Coatings Technol. 203 (2009) 3325-3331.

[48] J. B. Cambon, J. Esteban, F. Ansar, J. P. Bonino, V. Turq, S. H. Santagneli, C. V. Santilli, S. H. Pulcinelli, Effect of cerium on structure modifications of a hybrid sol–gel coating, its mechanical properties and anti-corrosion behaviour, Mater. Res. Bull. 47 (11) (2012) 3170-3176.

[49] L. Sowntharya, S. Lavanya, G. R. Chandra, N. Y. Hebalkar, R. Subasri, Investigations on the mechanical properties of hybrid nanocomposite hard coatings on polycarbonate, Ceram. Int. 38 (5) (2012) 4221-4228.

[50] H. Rahimi, R. Mozaffarinia, A. H. Najafabadi, Corrosion and wear resistance characterization of environmentally friendly sol-gel hybrid nanocomposite coating on AA5083, J. Mater. Sci. Technol. 29 (7) (2013) 603-608.

[51] C. M. Chan, G. Z. Cao, H. Fong, M. Sarikaya, T. Robinson, L. Nelson, Nanoindentation and adhesion of sol-gel-derived hard coatings on polyester, J. Mater. Res. 15 (1) (2000) 148-154.

[52] L. Sowntharya, R. C. Gundakaram, K. R. C. Soma Raju, R. Subasri, Effect of addition of surface modified nanosilica into silica-zirconia hybrid sol-gel matrix, Ceram. Int. 39 (4) (2013) 4245-4252.

[53] F. Dolatzadeh, S. Moradian, M. M. Jalili, Influence of various surface treated silica nanoparticles on the electrochemical properties of SiO2/polyurethane nanocoatings, Corros. Sci. 53 (12) (2011) 4248-4257.

[54] L. Vivar Mora, S. Naik, S. Paul, R. Dawson, A. Neville, R. Barker, Influence of silica nanoparticles on corrosion resistance of sol-gel based coatings on mild steel, Surf. Coatings Technol. 324 (2017) 368-375.

[55] J. Malzbender, J.M.J. den Toonder, A.R. Balkenende, G. de With, Measuring mechanical properties of coatings: a methodology applied to nano-particle-filled sol-gel coatings on glass, Mater. Sci. Eng. R. 36 (2002) 47–103.

[56] W. Stober, A. Fink, E. Bohn, Controlled Growth of Monodisperse Silica Spheres in the Micron Size Range, J. Colloid Interface Sci. 26 (1968) 62–69.

[57] W. C. Oliver, G. M. Pharr, An improved technique for determining hardness and elastic modulus using load and displacement sensing indentation experiments, J. Mater. Res. 7 (6) (1992) 1564.

[58] A. Neville, C. Wang, Erosion-corrosion mitigation by corrosion inhibitors- An assessment of mechanisms, Wear, 267 (1-4) (2009) 195-203.

[59] K. J. Pascoe, An introduction to the properties of engineering materials, Springer, 1978.

[60] A. Leyland, A. Matthews, On the significance of the H/E ratio in wear control: a nanocomposite coating approach to optimised tribological behaviour, Wear 246 (2000) 1-11.

[61] G. Pintaude (2013). Introduction of the Ratio of the Hardness to the Reduced Elastic Modulus for Abrasion, Tribology - Fundamentals and Advancements, Dr. Jürgen Gegner (Ed.), InTech,. Available from: https://www.intechopen.com/books/tribology-fundamentals-and-advancements/introduction-of-the-ratio-of-the-hardness-to-the-reduced-elastic-modulus-for-abrasion

[62] G. M. Pharr, Measurement of mechanical properties by ultra-low load indentation, Mater. Sci. Eng. A. 253 (1/2) (1998) 151-159.

[63] L. Shen, L. Wang. T. Liu, C. He, Nanoindentation and morphological studies of epoxy nanocomposites, Macromol. Mater. Eng. 291 (2006) 1358-1366.

[64] R. B. Figueira, E. Callone, C. J. R. Silva, E. V. Pereira, S. Dirè, Hybrid coatings enriched with tetraethoxysilane for corrosión mitigation of hot-dip galvanized steel in chloride contaminated simulated concrete pore solutions, Materials, 10 (2017) 306.

[65] A. Shahryari, W. Kamal, S. Omanovic, The effect of surface roughness on the efficiency of the cyclic potentiodynamic passivation (CPP) method in the improvement of general and pitting corrosion resistance of 316LVM stainless steel, Mater. Lett. 2008, 62, 2906-3909.

[66] B. Elsener, A. Rota, H. Böhni, Impedance study on the corrosion of PVD and CVD titanium nitride coatings, Mater. Sci. Forum 44-45 (1989) 29-38.

[67] E. Barsoukov, J.R. Macdonald, Impedance Spectroscopy: Theory, experimental and applications, 2nd ed., John Wiley & Sons, 2005.

[68] M.G. Olivier, M. Poelman, Use of Electrochemical Impedance Spectroscopy (EIS) for the Evaluation of Electrocoatings Performances, in: Reza Shoja Razavi (Ed.), Recent Res. Corros. Eval. Prot., Intechopen, 2012.

[69] A. C. Ciubotariu, L. Benea, P. Ponthiaux, Corrosion resistance of zinc-resin hybrid coatings obtained by electro-codeposition, Arab. J. Chem. (2016).

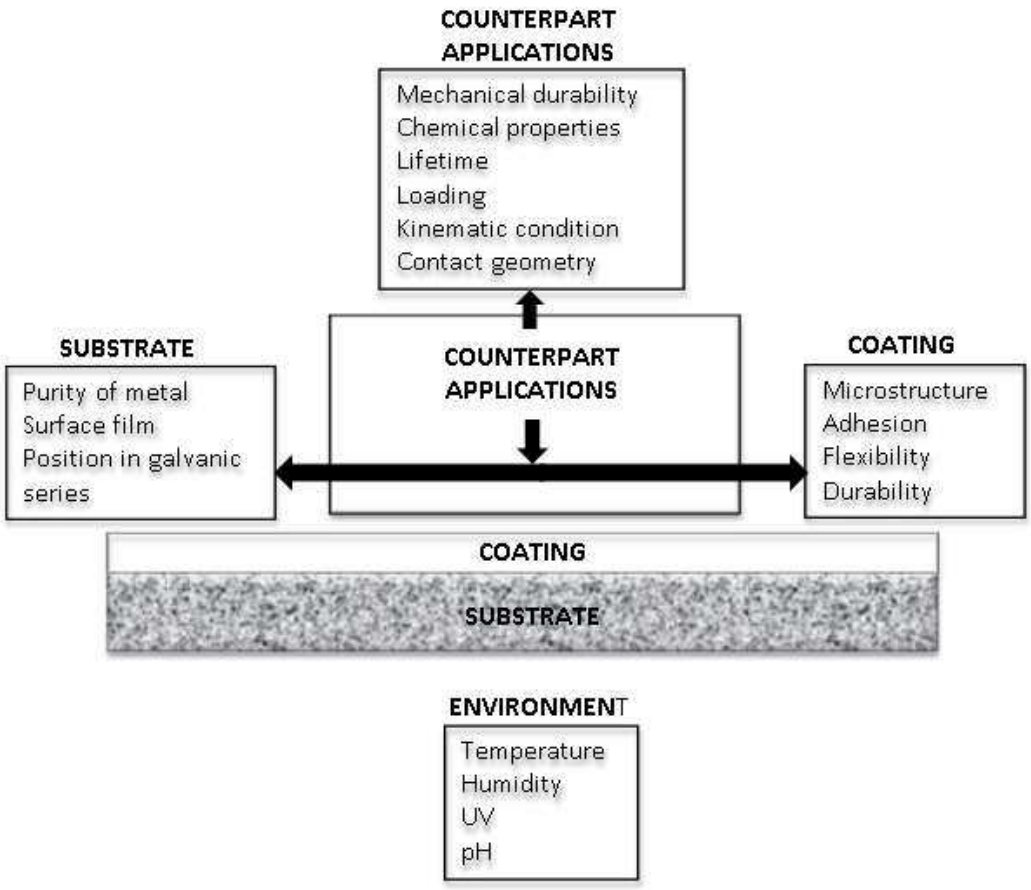

Figure 1. Factors affecting corrosion and coating durability 'Courtesy of TWI Ltd.'

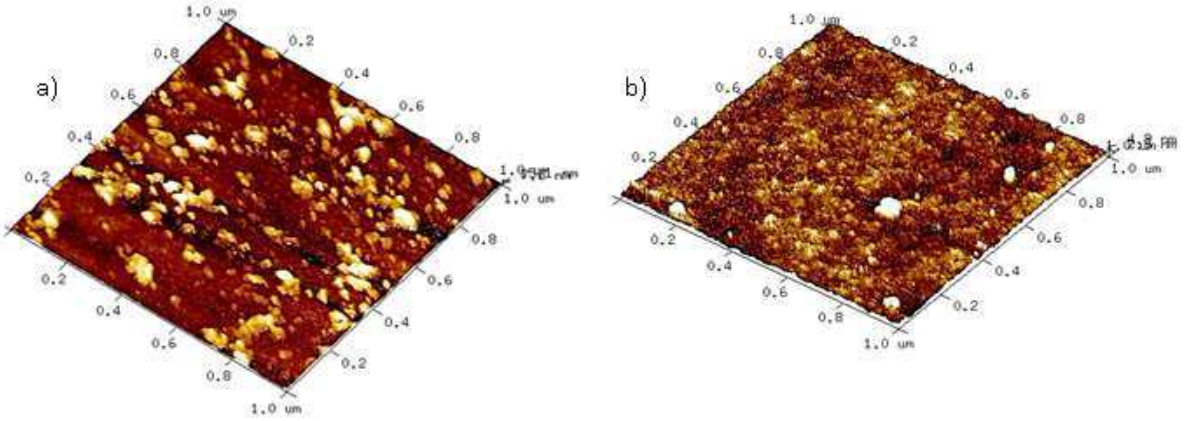

Figure 2. Topography images of coating matrix with a) unfunctionalised SiO_2 and b) functionalised SiO_2. 'Courtesy of TWI Ltd.'

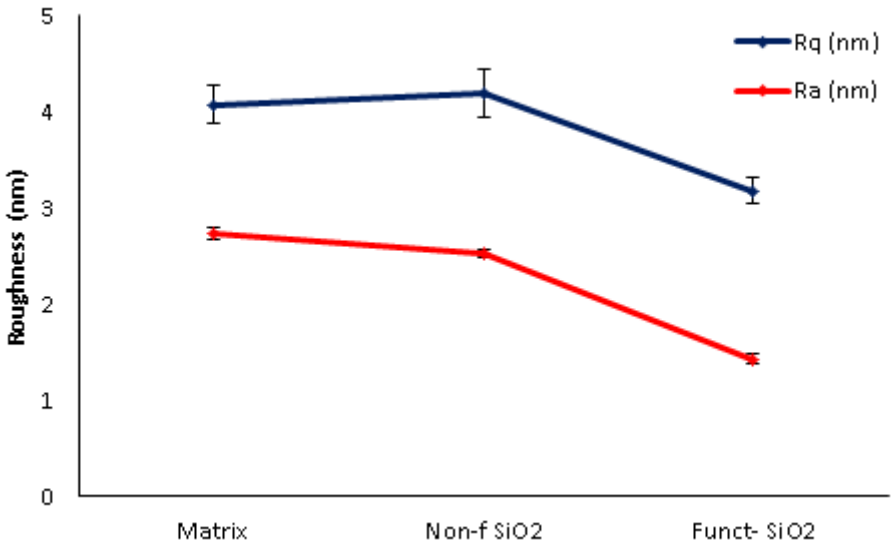

Figure 3. Surface roughness parameters, R_a and R_q measured using AFM 'Courtesy of TWI Ltd.'

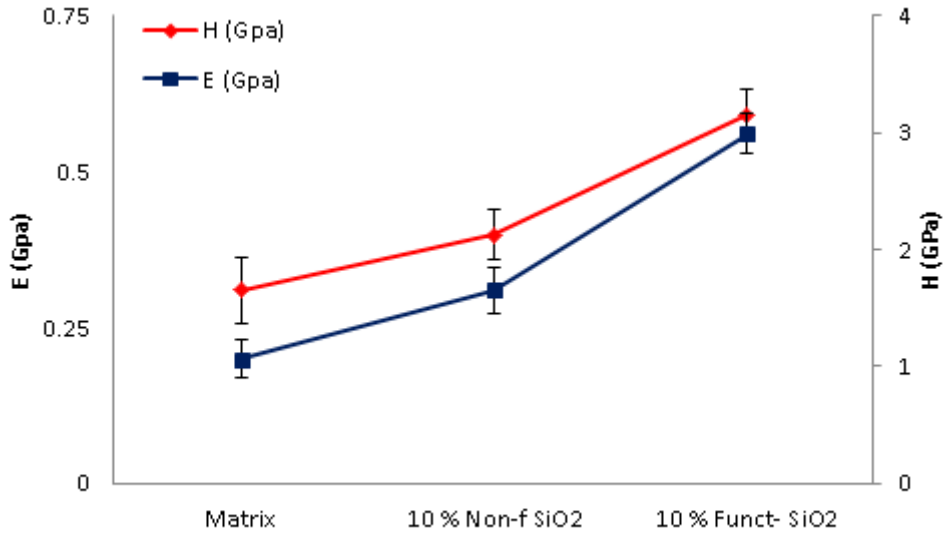

Figure 4. Young's modulus for all coating formulations 'Courtesy of TWI Ltd.'

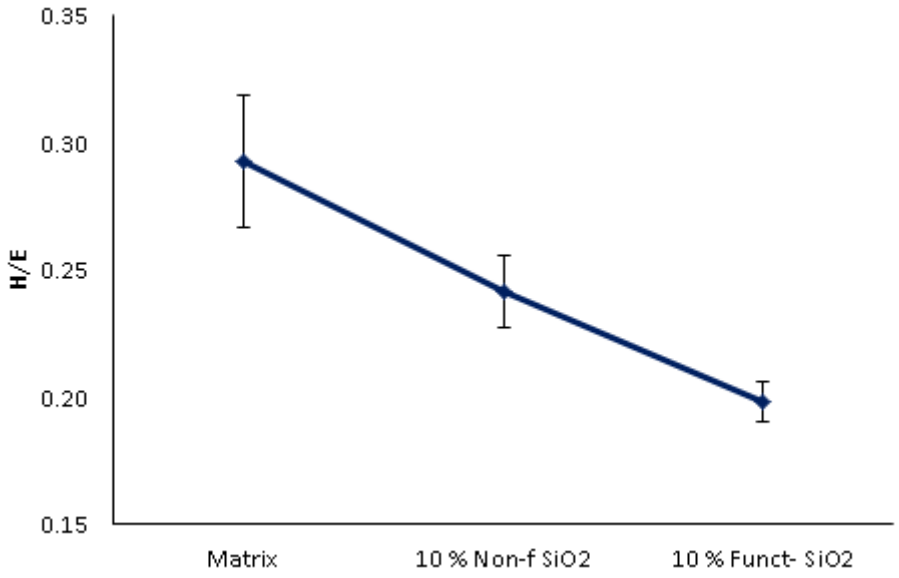

Figure 5. Brittleness indexes, H/E, for all formulations 'Courtesy of TWI Ltd.'

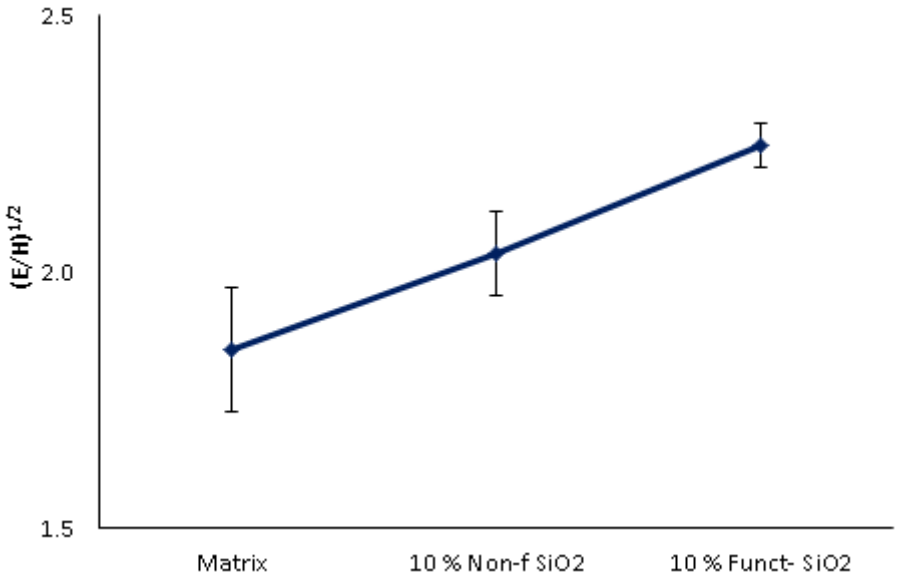

Figure 6. Evolution of the potential to resist fracture 'Courtesy of TWI Ltd.'

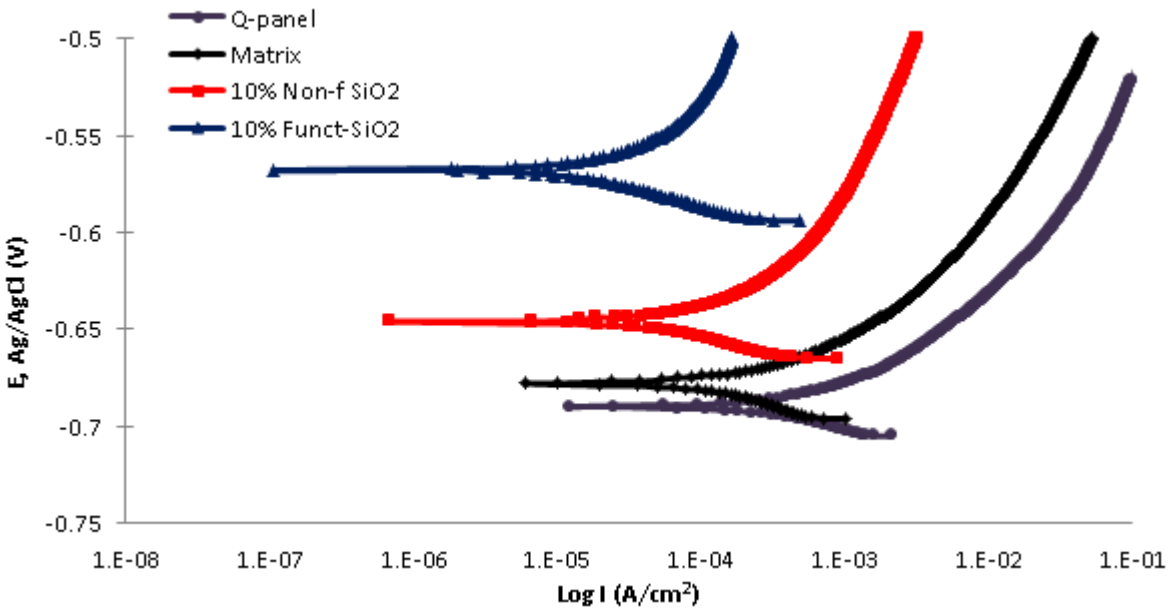

Figure 7. Potentiodynamic polarisation curves after 48h of immersion in 3.5 wt.% NaCl solution 'Courtesy of TWI Ltd.'

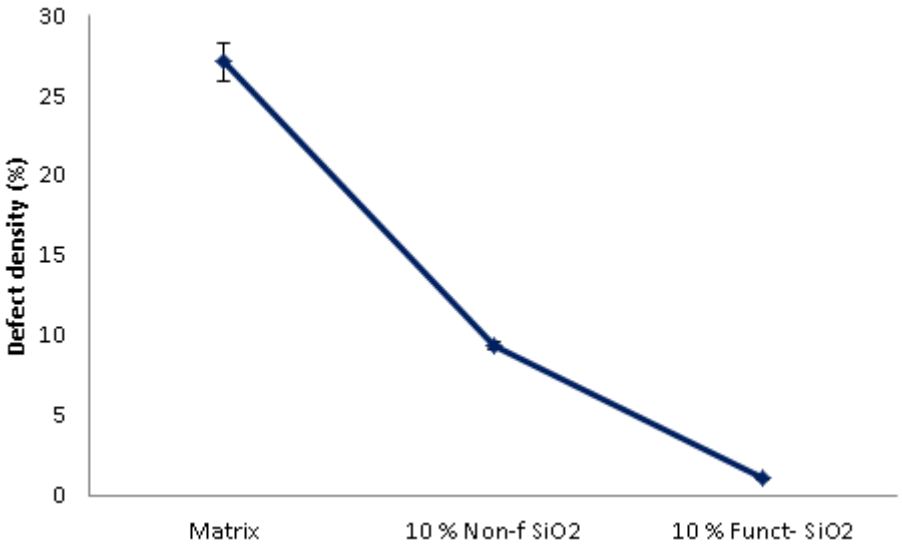

Figure 8. Defect density values after potentiodynamic polarisation 'Courtesy of TWI Ltd.'

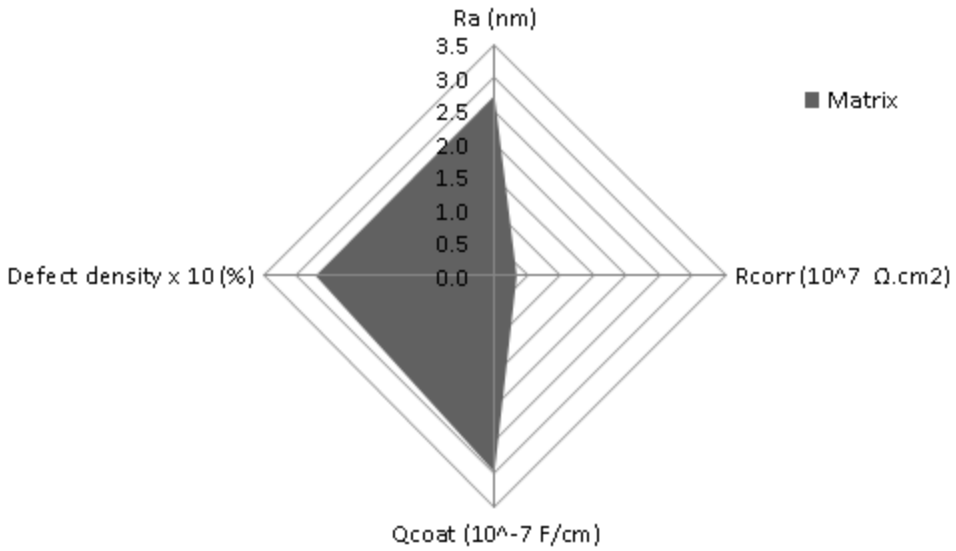

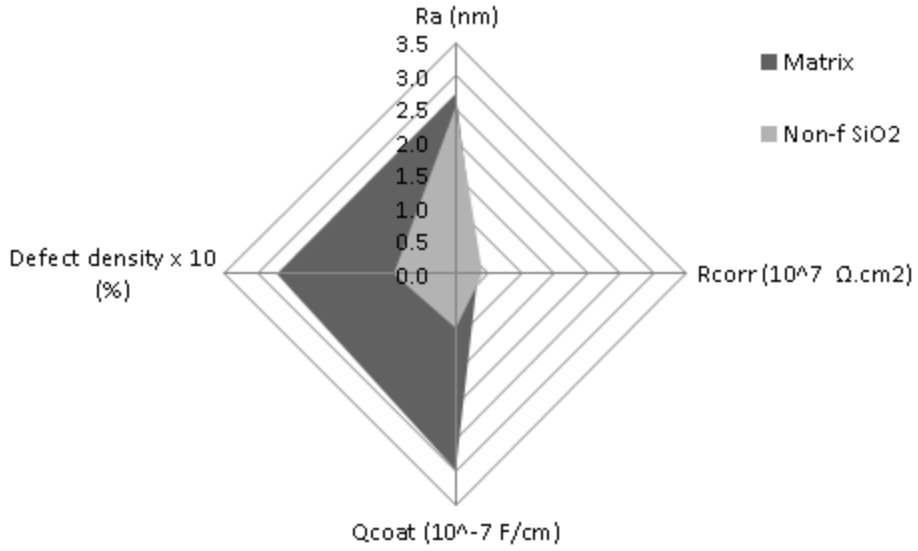

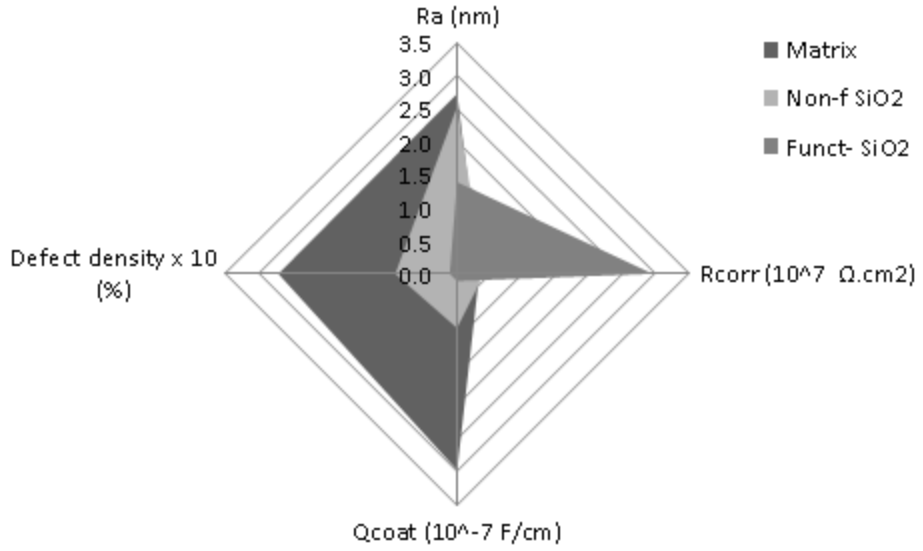

Figure 9. Influence of roughness on defect density, water uptake and corrosion resistance 'Courtesy of TWI Ltd.'

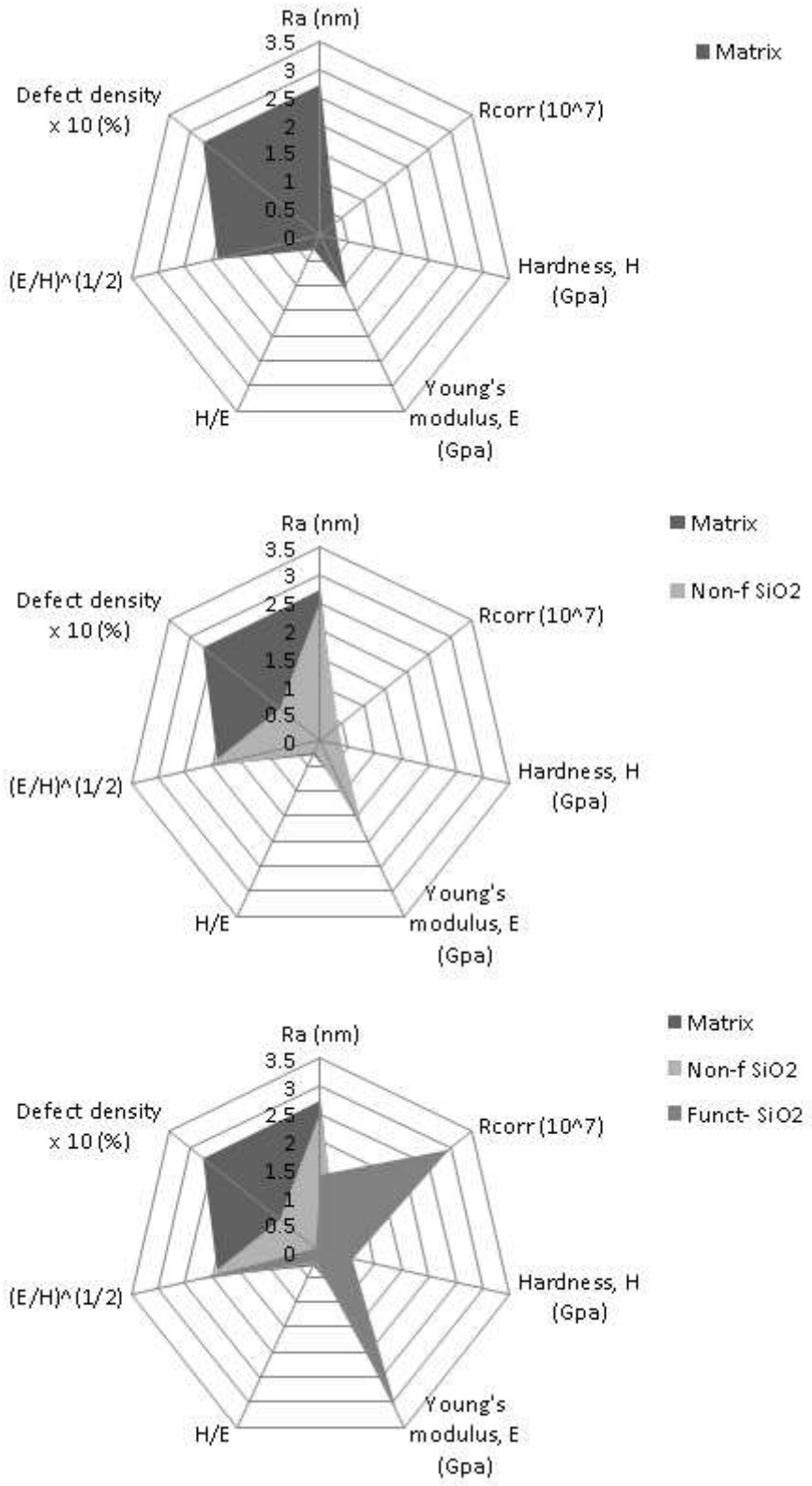

Figure 10. Evaluation of mechanical durability and corrosion resistance 'Courtesy of TWI Ltd.'

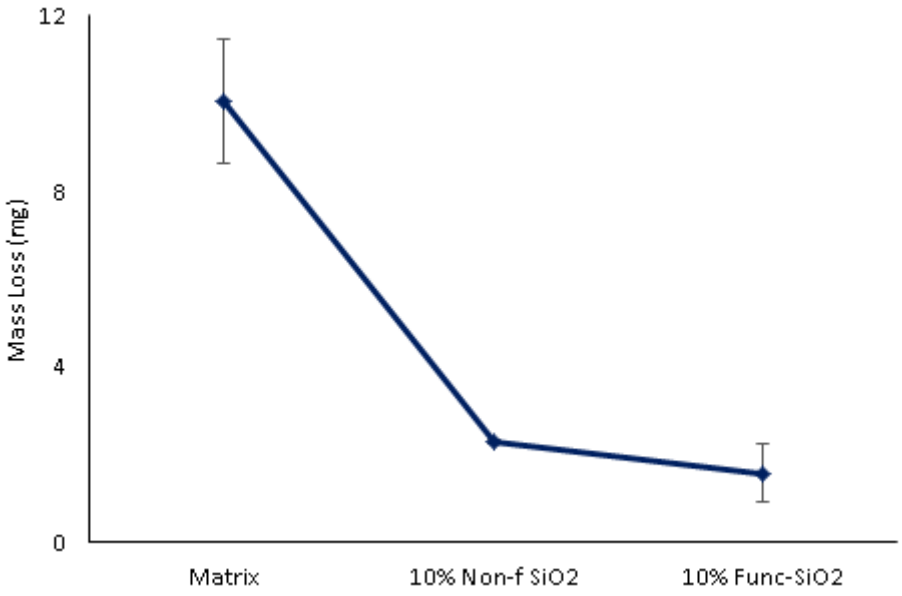

Figure 11. Erosion resistance of all formulations after 4-hour submerged impingement jet erosion tests at 15 m/s with a sand concentration of 1000 mg/L. 'Courtesy of TWI Ltd.'

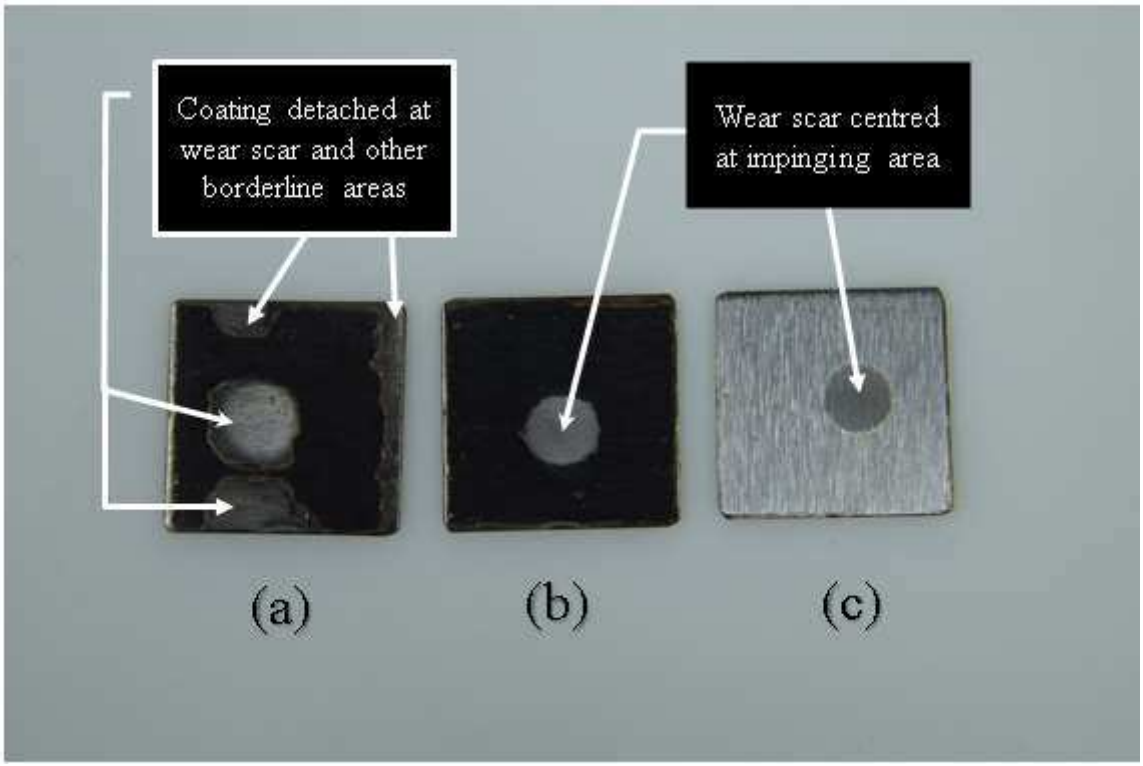

Figure 12. Surface morphology images of samples after 4-hours submerged impingement jet erosion tests at 15 m/s flow velocity, 1000 mg/L sand loading in a N_2 saturated environment for (a) sol-gel based matrix (b) matrix with 10 wt.% non-functionalised silica and (c) matrix with 10 wt.% functionalised silica. 'Courtesy of TWI Ltd.'

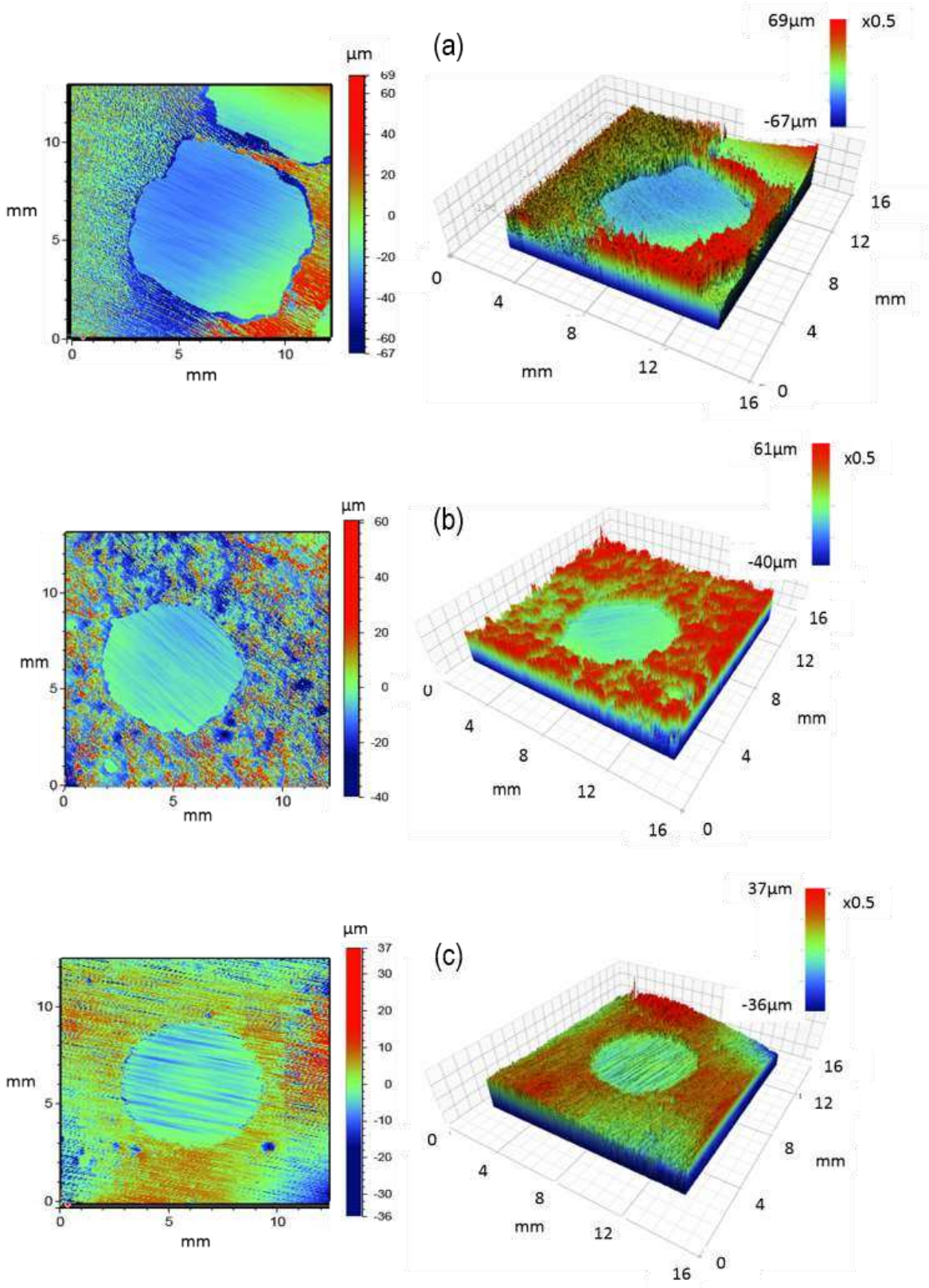

Figure 13. 2D and 3D surface profiles images after 4-hour erosion tests: (a) sol-gel based matrix (b) matrix with 10 wt.% non-functionalised silica and (c) matrix with 10 wt.% functionalised silica. 'Courtesy of TWI Ltd.'

Figure 1. Factors affecting corrosion and coating durability ‘Courtesy of TWI Ltd.’

Figure 2. Topography images of coating matrix with a) unfunctionalised SiO_2 and b) functionalised SiO_2. ‘Courtesy of TWI Ltd.’

Figure 3. Surface roughness parameters, R_a and R_q measured using AFM ‘Courtesy of TWI Ltd.’

Figure 4. Young’s modulus for all coating formulations ‘Courtesy of TWI Ltd.’

Figure 5. Brittleness indexes, H/E, for all formulations ‘Courtesy of TWI Ltd.’

Figure 6. Evolution of the potential to resist fracture ‘Courtesy of TWI Ltd.’

Figure 7. Potentiodynamic polarisation curves after 48h of immersion in 3.5 wt.% NaCl solution ‘Courtesy of TWI Ltd.’

Figure 8. Defect density values after potentiodynamic polarisation ‘Courtesy of TWI Ltd.’

Figure 9. Influence of roughness on defect density, water uptake and corrosion resistance ‘Courtesy of TWI Ltd.’

Figure 10. Evaluation of mechanical durability and corrosion resistance ‘Courtesy of TWI Ltd.’

Figure 11. Erosion resistance of all formulations after 4-hour submerged impingement jet erosion tests at 15 m/s with a sand concentration of 1000 mg/L. ‘Courtesy of TWI Ltd.’

Figure 12. Surface morphology images of samples after 4-hours submerged impingement jet erosion tests at 15 m/s flow velocity, 1000 mg/L sand loading in a N_2 saturated environment for (a) sol-gel based matrix (b) matrix with 10 wt.% non-functionalised silica and (c) matrix with 10 wt.% functionalised silica. ‘Courtesy of TWI Ltd.’

Figure 13. 2D and 3D surface profiles images after 4-hour erosion tests: (a) sol-gel based matrix (b) matrix with 10 wt.% non-functionalised silica and (c) matrix with 10 wt.% functionalised silica. ‘Courtesy of TWI Ltd.’

Table 1. Comparison of mechanical properties for the nanocoatings compared to the base matrix 'Courtesy of TWI Ltd.'

	Hardness (H, GPa)	H change relative to matrix	Young's modulus (E, GPa)	E change relative to matrix	Brittleness index (H/E)	H/E change relative to matrix
Matrix	0.311 ± 0.053	-	1.063 ± 0.161	-	0.292 ± 0.026	-
Non-f SiO_2	0.399 ± 0.040	9%	1.653 ± 0.197	62%	0.241 ± 0.014	5%
Funct-SiO_2	0.591 ± 0.040	28%	2.988 ± 0.172	202%	0.198 ± 0.008	9%